Chemical Physics 374 (2010) 126–130

Contents lists available at ScienceDirect

Chemical Physics

journal homepage: www.elsevier.com/locate/chemphys

2-D modeling of dual-mode acoustic phonon excitation of a triangular nanoplate

Po-Tse Tai [a], Pyng Yu [a], Jau Tang [a,b,*]

[a] Research Center for Applied Sciences, Academia Sinica, Taipei, Taiwan
[b] Institute of Photonics, National Chiao-Tung University, Hsinchu, Taiwan

ARTICLE INFO

Article history:
Received 22 April 2010
In final form 9 July 2010
Available online 14 July 2010

Keywords:
Ultrafast phenomena
Coherent phonon
Photoacoustic effects
Laser heating

ABSTRACT

In this theoretical work, we investigated coherent phonon excitation of a triangular nanoplate based on 2-D Fermi–Pasta–Ulam lattice model. Based on the two-temperature model commonly used in description of laser heating of metals, we considered two kinds of forces related to electronic and lattice stresses. Based on extensive simulation and analysis, we identified two major planar phonon modes, namely, a standing wave mode related to the triangle bisector and another mode corresponding to half of the side length. This work elucidates the roles of laser-induced electronic stress and lattice stress in controlling the initial phase and the amplitude ratio between these two phonon modes.

1. Introduction

Recently, studies of laser heating, ablation and annealing by pulsed lasers have been extended from bulk materials to nanomaterials. Laser-excited coherent acoustic oscillations have been widely observed in the nanoparticles or nanoscale thin films. Such oscillation periods can be directly or indirectly measured by optical pump-probe techniques [1–11] or ultrafast electron crystallography [12]. Due to fast thermal conduction and ballistic motion of laser-heated hot electrons, the thermal stress due to heated electron or lattice usually has a deep penetration depth and a long time profile. Therefore, in most cases only the lowest frequency modes corresponding to the standing waves are excited. In an experimental study of laser-heated nanoprisms two planar acoustic phonon modes were observed. In our previous study [13], we applied 1-D Fermi–Pasta–Ulam model (FPU) to describe ultrafast structural dynamics of a thin film. Here, we consider 2-D FPU model to investigate the dynamics of a triangular nanoplate. Although in an actual 3-D nanoprism, there is one additional dimension as thickness, our 2-D simplification could capture most of the major relevant behavior as long as the thickness is much smaller than other two dimensions. Based on such 2-D model, we hope to explain: (1) how the thermal stress of hot electron excites the totally symmetric mode; (2) the relationship between the totally symmetric mode and the triangle size; and (3) the origin for a $\pi/2$ phase difference between the breathing mode and the totally symmetric mode.

2. 2-D Fermi–Pasta–Ulam model

In previous studies [14,15], we employed a combined model based on the two-temperature model (TTM) and 1-D FPU model to treat heat transfer and structural dynamic in laser-heated metallic thin films. Such a modeling approach provides a better description of laser-induced ultrafast structural dynamics than the phenomenological single harmonic oscillator model. The commonly used single harmonic oscillator model assumes the whole thin film behaves as an oscillator, and is certainly not suitable to describe excitation of two planar modes of a nanoplate. In this study of ultrafast structural dynamics of a nanoplate, we focus on impulse induced 2-D dynamics instead of full treatment with a combined 2-D TTM and 2-D FPU model, which would be much more complicated and CPU demanding. We shall apply the 2-D FPU model with two types of impulsive forces to capture the major physical essence of TTM with electron and lattice subsystems. One type of force, direct force, corresponds to the change of the electron temperature which, according to TTM, has a very short duration with a fast rising time constant and a falling time constant on the order of ps. The other type of force, indirect force, corresponding to the phonon temperature, according to TTM, has a slightly slower rising time than the electron temperature but a much longer decay time and usually on the order of ns. Therefore, in this study we use 2-D FPU model with the presence of both forces, or direct and indirect forces as called by others [16,17], to treat the ultrafast planar lattice dynamics of a triangular nanoplate. These two types of impulsive forces can be expressed as

$$\begin{aligned} F_D &= w_1 \times \exp(-t/\tau_{e-ph}) \times \exp(-z/\lambda_1) \\ F_I &= w_2 \times \lfloor 1 - \exp(-t/\tau_{e-ph}) \rfloor \times \exp(-z/\lambda_2) \end{aligned} \quad (1)$$

* Corresponding author at: Research Center for Applied Sciences, Academia Sinica, Taipei, Taiwan. Tel.: +886 2 2652 5186; fax: +886 2 2782 6672.
E-mail address: jautang@gate.sinica.edu.tw (J. Tang).

0301-0104/$ - see front matter © 2010 Elsevier B.V. All rights reserved.
doi:10.1016/j.chemphys.2010.07.010

where F_D and F_I represent the effective direct and indirect forces, w_1 and w_2 are the force magnitudes, τ_{e-ph} is the characteristic time constant of electron–phonon interactions, and λ_1 and λ_2 are the penetration depth of the direct and indirect forces. The thermal stress generation by the temperature change could be expressed as $\sigma = \sigma_e + \sigma_l = -\gamma_e C_e T_e \times \Delta T_e - \gamma_l C_l \times \Delta T_l$, where σ_e and σ_l are the stress caused by hot electrons and lattice, or referred to as direct and indirect forces here, $C_l = 3.5 \times 10^6\ \mathrm{Jm^{-3}\,K^{-1}}$ and $C_e = 66\ \mathrm{Jm^{-3}\,K^{-2}}$ are the lattice and electron heat capacity, $\gamma_e = 0.97$ and $\gamma_l = 2.23$ are Grüneisen parameter for electron and lattice, T_e and T_l are electron and lattice temperatures, and ΔT_e and ΔT_l are the electron and phonon temperature change for silver nanoprisms, respectively [18]. When the maximum electron and lattice temperatures were specified, the relationship between F_D and F_I can be determined. From the two-temperature model, we can estimate the maximum electron temperature through τ_{e-ph} [19,20]. The maximum electron temperature is given by $\tau_{e-ph} \times g/C_e$, where the electron–phonon coupling constant $g = 3 \times 10^{16}\ \mathrm{Wm^{-3}\,K^{-1}}$, and τ_{e-ph} was determined to be 2.79 ps [4]. When the initial temperature is 300 K, we estimated the maximum electronic temperature to be about 1268 K. From the energy conservation, the maximum temperature of lattice was obtained to be 323 K. Therefore, the ratio between the direct and indirect forces is $w_1/w_2 = 0.43$, and this value was fixed in our simulation.

A silver nanoprism is known to grow on the (1 1 1) plane of an f.c.c. structure [21,22]. A planar triangle on the (1 1 1) plane is shown in Fig. 1. A spring is drawn to represent the interaction between two adjacent atoms. Because the metallic atom in a solid experiences non-directional forces, we could consider here a spherical harmonic potential. Although the anharmonic potential, such as Morse potential, could be considered in the FPU model, our use of a harmonic potential represents the truncation of a Taylor series expansion of any harmonic potential to the 2nd order term. Because the magnitude of vibrational amplitude is rather small, the anharmonic effects could be neglected here. Laser heating of silver nanoparticles is through the dipole plasmon resonance [4], and the impulsive thermal stress is due to sudden changes of thermal gradient [13–15]. In the nanoprism, due to the fact that the apex enhances the localized field, the three sharp tips have higher light absorption than the residual part [23]. In particular, the tip along the laser polarization has enhanced localized field significantly [23,24]. Since the excitation laser is polarized, there is usually one tip to be more parallel to the laser polarization than the others in a randomly oriented nanoprism. For simplicity, we shall assume the laser polarization along the z-axis and first consider an impulsive force in the same direction as shown in Fig. 1(a), and we shall neglect the influence of two other forces of Fig. 1(b) which will be discussed later. Assuming an impulsive force along the z-direction, according to the FPU model one has

$$
\begin{aligned}
\frac{dS_n}{dt} &= \frac{P_n}{m} \\
\frac{dP_1}{dt} &= F_1 - \gamma P_1 - m\omega^2(S_1 - S_2) - m\omega^2(S_1 - S_3) \\
\frac{dP_2}{dt} &= F_2 - \gamma P_2 - m\omega^2(S_2 - S_1) \\
&\vdots \\
\frac{dP_5}{dt} &= F_5 - \gamma P_5 - m\omega^2(S_5 - S_2) - m\omega^2(S_5 - S_3) - m\omega^2(S_5 - S_4) \\
&\quad - m\omega^2(S_5 - S_6) - m\omega^2(S_5 - S_8) - m\omega^2(S_5 - S_9) \\
&\vdots
\end{aligned}
\tag{2}
$$

where S_n is the atomic displacement for the nth atom, F_n is the impulsive force, which is consist of both direct and indirect forces due to thermally induced stress on electrons and lattice, P_n is the momentum, γ is the damping factor, and $m\omega^2$ is the force constant. According to our previous work using a simplified 1-D FPU model, the effective angular frequency ω is equal to v_s/l, where v_s is the sound velocity and l is the bond distance. In this simulation, we used $m = 17.92 \times 10^{-26}$ kg, $m\omega^2 = 14.29$ N/m, lattice constant $l = 4.09$ Å, sound velocity $v_s = 3650$ m/s for the silver nanoprism. At time zero, the atoms are assumed to be at equilibrium position. Except for those atoms at the boundary, each atom is connected to six adjacent atoms, and the equation of motion for each atom is described by Eq. (2). In our computer algorithm, we have specially dealt with those boundary atoms as shown in Eq. (2), according to their specific couplings to adjacent atoms. The Runge–Kutta method was employed to numerically solve the above coupled equation. In most of the data analysis of coherent acoustic oscillations, only a damped single harmonic oscillator was considered [16,17]. In contrast, our approach of using the 2-D FPU model allows us to quantitatively simulate the structural dynamics to gain better physical understanding of its shape- or size-dependence.

3. Simulation results and discussion

The effective direct and indirect forces are induced by changes in the electron and phonon temperatures, respectively. Since the optical field directly heats up the electrons at the beginning, the initial hot electron distribution, which is the cause for the direct force, is controlled by the local optical field. From the previously study [23,24], the sharp tip could enhance the localized field in the range of several tens of nanometer. Therefore, we expect the order of the magnitude for λ_1 to be around the several tens of nanometer. Afterward, the hot electrons rely on the ballistic motion and fast thermal diffusion to redistribute their energy to colder elec-

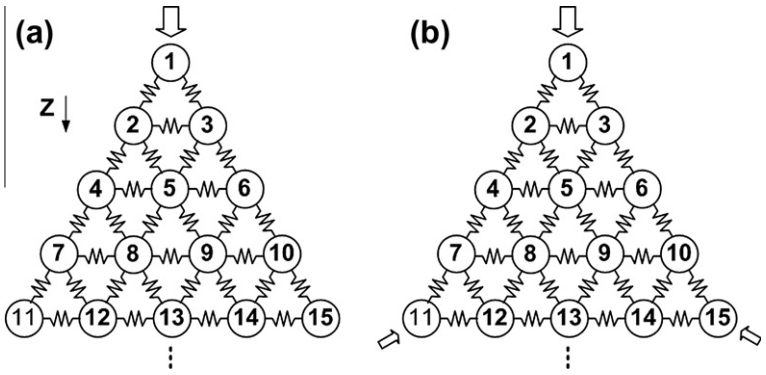

Fig. 1. A schematic diagram showing a triangular plate on (1 1 1) plane of an f.c.c. structure. Each atom is connected to the nearest neighbors by springs. The arrows indicate the direction of impulsive thermal stress.

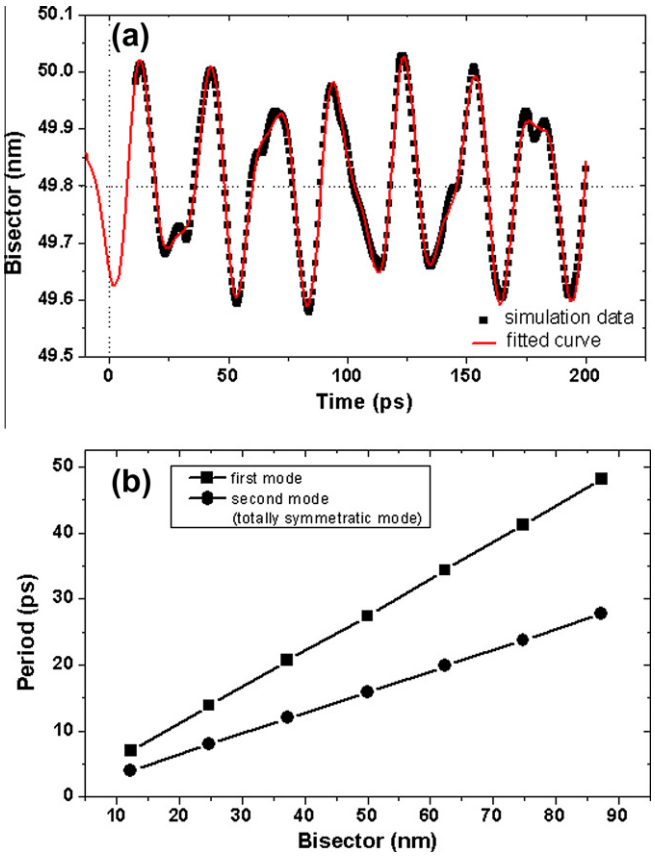

Fig. 2. (a) Excitation of acoustic oscillations of a triangular plate with 49.8 nm bisector. (b) The oscillation periods versus bisector height. The simulated dot curves were fitted using $T_1 = 27.4$ ps, $T_2 = 15.8$ ps, $\phi_1 = 181°$, $\phi_2 = 85°$ and amplitude ratio $B/A = 0.387$. The ratio of two frequencies in the same triangle size is close to $\sqrt{3}$.

trons elsewhere, and then these hot electrons transfer the heat to phonons. Since the phonons are heated up indirectly by a laser heating pulse, the phonon temperature gradient, which induces the indirect force, is more uniform than the initial electron temperature distribution. For a comparison with experiment results [4], we used $\lambda_1 = 40$ nm for the direct force and $\lambda_2 = 1$ μm for the indirect force, and the electron–phonon energy transfer time constant of 2.79 ps. Considering a triangle with a bisector of 49.8 nm, the excitation acoustic oscillations shown in Fig. 2(a) correspond to a breathing mode vibration involving the bisector. The dot curve represents our simulation results, and the red line represents the fitted data using[1]

$$A \times \cos\left(\frac{2 \times \pi \times t}{T_1} + \phi_1\right) + B \times \cos\left(\frac{2 \times \pi \times t}{T_2} + \phi_2\right) \quad (3)$$

where A and B are the amplitude for different modes, T_1 and T_2 are the corresponding oscillation periods, and ϕ_1 and ϕ_2 are the corresponding initial phases. To reduce the number of fitting parameters, we consider no damping in Eq. (2). From the fits, we found that $T_1 = 27.4$ ps, $T_2 = 15.8$ ps, $\phi_1 = 181°$ and $\phi_2 = 85°$. The fitted period of the first mode can be well approximated by $2L/v_s$, where $L = 50$ nm which is the triangle bisector. The fitted second mode $L = 28.8$ nm corresponds to the half triangle size. Similar two mode oscillations have also been observed for different triangle bisectors, as shown in Fig. 2(b). The oscillation periods of these two modes are in quantitative agreement with the breathing mode involving the triangle bisector and the half triangle size. Therefore, the ratio of these two frequencies for the same triangle size is close to $\sqrt{3}$. In addition, the phase difference was found to be about $\pi/2$ between these two modes. In the experiments of triangular plates two different planer modes with the similar frequency ratio were observed [4]. The breathing mode, or called the first mode here, depends on the lateral dimension. On the other hand, the totally symmetric mode, or called the second mode here, also vibrates on the plane but could affect the thickness dimension. A change of the thickness affects the imaginary part of the dielectric constant. From their analysis as shown in Fig. 4 from Ref. [4], the first mode has a one-step phase change and the second mode has a two-step change around the surface plasmon resonance (SPR) due to the Kramers–Kronig relationship between real and imaginary part of dielectric constant, where each step has a π phase change [25]. In the experimental results, the initial phase of the first mode should be either 0 or π, and the second mode is either $\pi/2$ or $3\pi/2$. From the fitted phase to our simulated data, we obtained a phase about π (181°) for the first mode and about $\pi/2$ (85°) for the second mode. Direct comparison of the experimental observation [4] and Fig. 2 indicates that our simulations for a triangle plate not only yield correctly the periods but also the phases for two different modes as observed experimentally.

The acoustic oscillation could be excited by F_D or by F_I as shown in Fig. 3(a and b), respectively. We decompose the curve in Fig. 2(a) into two physical parts. We expect the periods would be the same as the period excited by $F_D + F_I$, because the same force constant was used in the FPU model. Here, we point out that the amplitude ratio of two modes $B/A = 0.06$ in Fig. 3(a) and $B/A = 0.003$ in

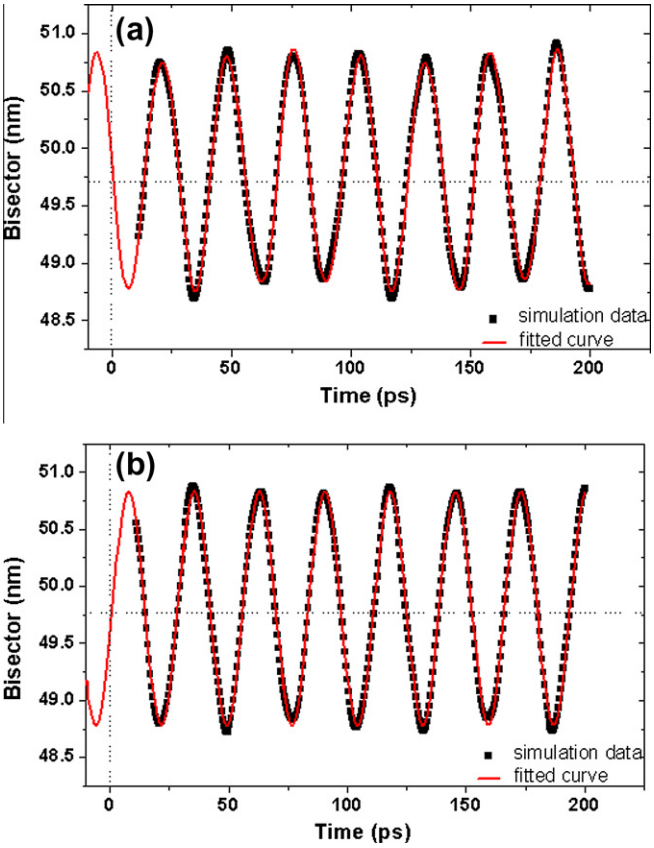

Fig. 3. (a) Excitation of acoustic oscillations by F_D. The fitted periods of the oscillations are $T_1 = 27.4$ ps, $T_2 = 15.8$ ps, $\phi_1 = 87.2°$, $\phi_2 = 82°$ and $B/A = 0.06$, showing the 2nd mode is weaker than the 1st mode. (b) Excitation of acoustic oscillations by F_I with fitted $\phi_1 = 260°$, $\phi_2 = 165°$ and $B/A = 0.003$, showing a much weaker 2nd mode.

[1] For interpretation of color mentioned the reader is referred to the web version of the article.

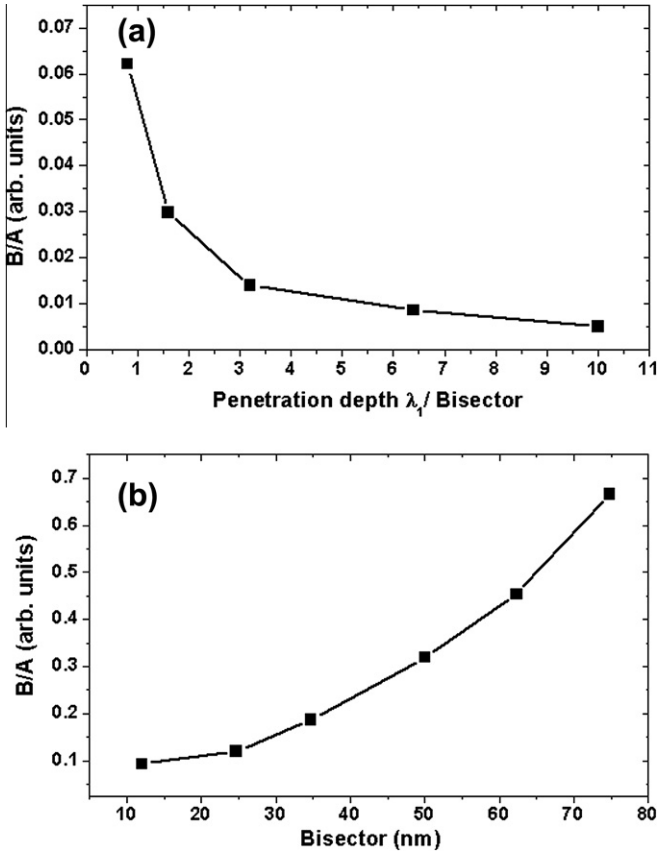

Fig. 4. (a) The amplitude ratio versus penetration depth. (b) The amplitude ratio versus triangular bisector height.

Fig. 3(b). At the fixed ratio of force magnitude $w_1/w_2 = 0.43$, the amplitude of first mode excited by F_D or by F_I is almost the same and the amplitude of the second mode excited by F_I is one order of magnitude smaller than that of the mode excited by F_D. Therefore, we concluded that F_D is the major force to excite the second mode.

Here, we described a physical explanation to the cause of the 90° phase difference, which has been an important issue that has not been understood until now. The initial phase of the first mode is $\phi_1 = 87.2°$ as excited by F_D, in contrast to $\phi_1 = 260°$ as excited by F_I. Since the two first modes excited by F_D and by F_I are nearly out of phase, the superimposed oscillations exhibit destructive interference. It is simple to determine that the initial phase of the superposed oscillations is around 174°, based on the sum-to-product trigonometric formula. We also obtained an initial phase of $\phi_2 = 82°$ for the second mode as excited by F_D, in comparison to $\phi_2 = 165°$ as excited by F_I. The superposition of these two modes yields nearly the same oscillations as those excited by F_D. The reason is that F_D is the major force to excite the second mode as mentioned earlier. The initial phase of the superposed oscillations of the second modes is around 82°. Therefore, we conclude that F_D and F_I cause superimposed oscillations with about 90° of phase difference between the first mode and the second mode.

In the pump-probe experiment, since the very short-time changes (within a few ps) in the transient optical absorption is dominated by the hot electron dynamics, we need to remove a large smoothly decaying component in the data curve to extract longer time oscillatory patterns representing coherent acoustic vibration. In our model fitting and data analysis, we only fit the longer time oscillations. Now, we would like to discuss the relative amplitude of the first and the second mode. No matter how the oscillations are excited by either F_D or by F_I, the first mode is dominant and the amplitude of the first mode is two or three orders of magnitude greater than that of the second mode. As shown in Fig. 3(a and b), this weaker second mode could only cause small modulations on the first mode. Since between the first modes excited by F_D and by F_I are out of phase, even though the second mode is rather weak, it is still noticeable when the acoustic oscillations are excited by $F_D + F_I$ as shown in Fig. 2(a). The fitted amplitude ratio of $B/A = 0.31$ was obtained. In comparison with the results from the work by Bonacina et al. [4], the ratio of these two modes (B/A) is from 1/3 to 1/4 around SPR. Therefore, our model provides an amplitude ratio which is in good agreement with the experimental results.

As discussed earlier, F_D is the primary force to excite the second mode. Two variables could affect F_D, namely, the time constant of electron–phonon interactions τ_{e-ph} and the penetration depth. After extensive tests using τ_{e-ph} ranged from 85 fs to 2 ps, the initial phase and B/A were found to remain unchanged as shown in Fig. 3(a), and the amplitude has not changed more than 19%. However, the second variable λ_1, the penetration depth, affects the amplitude much more. If one scales up λ_1 10 times, the amplitude decreases about five times. The force difference between adjacent atoms, force gradient, is the major factor in producing acoustic oscillations instead of the force itself [13–15]. A greater λ_1, or a smaller force gradient in the nanoparticles, would yield smaller vibration amplitude. The amplitude ratio, B/A, versus penetration depth of force is shown in Fig. 4(a). The second mode appears to become less important if the penetration depth becomes greater than the bisector height. At a small force gradient it will be more difficult to excite and observe the second mode for a relatively small triangular nanoplate. As shown in Fig. 4(a), B/A is less than 0.01 when the bisector is three times smaller than the penetration depth. Therefore, simulation results in Fig. 4(b) illustrate the relationship between the triangular bisector and the amplitude ratio of two modes. This result is directly related to the experimental observation. In our recent experiment [26], the second mode is hardly observed in triangular plates with 31 nm for the bisector height. As the triangle bisector increases, a large deviation appears between the experimental result and the damped sinusoidal pattern observed by Hartland and co-workers [6]. It means that the second mode becomes more clear and detectable for large triangular plates. Such a conclusion is consistent with our simulation results.

Since the nanoprisms in solution have random orientations, the impulsive thermal force is certainly not as shown in Fig. 1(a). The plasmonic absorption of an incident laser pulse by a nanoprism is intensified at the three vertexes but the laser polarization induces

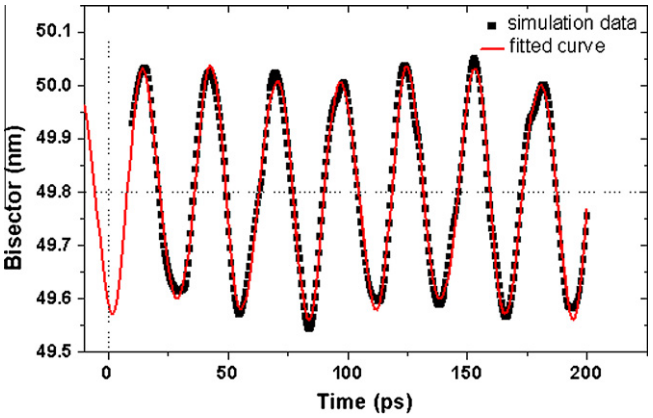

Fig. 5. Excitation of acoustic oscillations of a triangular plate by impulsive forces along three directions as shown in Fig. 1(b). The simulated dot curves were fitted using $\phi_1 = 165°$, $\phi_2 = 85°$ and an amplitude ratio $B/A = 0.095$.

different absorption at each tip [23]. Here, we include two weaker impulsive forces from two other directions which are 20% of the main force as shown in Fig. 1(b). The resultant coherent acoustic oscillations upon such three directional impulsive forces are shown in Fig. 5. We obtained a fitted amplitude ratio $B/A = 0.095$ and a phase difference of 80°, where 165° is the phase for first mode and 85° for second mode. Since the additional two small forces have a decreased force gradient, a relatively weak second mode was observed as compared to only one main force in the z-axis.

4. Conclusions

In conclusion, we extended the usual 1-D FPU model to 2-D to treat planar coherent acoustic phonon excitation in a triangular nanoplate. We considered two kinds of impulsive forces, namely, F_D and F_I, representing the thermal stress from laser-heated electrons and lattice. Using a specific example, we identified two planar phonon modes with a $\pi/2$ phase difference, representing a breathing mode and a totally symmetric mode. They correspond to standing waves related to the bisector height and half of the side length, respectively. The simulation results agree well with the experimental observation [4], and this study allows us to elucidate the roles of F_D and F_I in the coherent phonon excitation, and to explain the origin of the observed $\pi/2$ phase difference between these two modes. F_D is found to play the major role for excitation of the second mode. In contrast, both F_D and F_I contribute to the excitation of the first mode with nearly the same amplitude but opposite phase. As illustrated in Fig. 2(a), the destructive interference cancels each other's contribution to make the second mode appear more prominent. We have found that the amplitude of the acoustic oscillations depends on the non-uniform distribution of the impulsive force F_D. If the force is more spatially uniform, the amplitude of the first mode decreases, and the amplitude for the second mode decreases even more rapidly. Therefore, for a smaller triangular nanoplate or for a deeper force penetration, the excitation and detection of the second mode would become much difficult.

We do not believe that the temperature distribution within the laser-heated nanoprisms is uniform and isotropic. Otherwise, the stress caused by the sudden temperature changes would be uniform across the whole nanoparticle, implying that each atom would move in the same way and same speed [14]. If there is no relative speed difference between atoms, periodic expansion and contraction would not occur. We believe that although the temperature distribution in a nanoprism caused by laser heating is very close to uniformity, there exist small temperature variations within the nanoplate to result in multi-mode excitations. The simplified approach used here, using 2-D FPU model with two kinds of impulsive forces to represent the electronic and lattice stresses, allows us to capture the most relevant behavior observed in laser-heated nanoprisms. In the future, we plan to conduct a full treatment with a combined 3-D TTM and 3-D FPU model, which is certainly much more CPU demanding by several orders of magnitude.

Acknowledgement

J. Tang thanks the support of the Academia Sinica and National Science Council of Taiwan under the Program No. 98-2221-E-001-019. P.T. Tai acknowledges National Science Council for providing post doc fellowship.

References

[1] J.H. Hodak, A. Henglein, G.V. Hartland, J. Phys. Chem. B 104 (2000) 9954.
[2] C. Voisin, N. Del Fatti, D. Christofilos, F. Vallee, J. Phys. Chem. B 105 (2001) 2264.
[3] R. Taubert, F. Hudert, A. Bartels, F. Merkt, A. Habenicht, P. Leiderer, T. Dekorsy, New J. Phys. 9 (2007) 376.
[4] L. Bonacina, A. Callegari, C. Bonati, F.V. Mourik, M. Chergui, Nano Lett. 6 (2006) 7.
[5] N. Okada, Y. Hamanaka, A. Nakamura, I. Pastoriza-Santos, L. Liz-Harzan, J. Phys. Chem. 108 (2004) 8751.
[6] M. Hu, H. Petrova, X. Wang, G.V. Hartland, J. Phys. Chem. B 109 (2005) 14426.
[7] H. Petrova, C.H. Lin, S. de Liejer, M. Hu, J.M. McLellan, A.R. Siekkinen, B.J. Wiley, M. Marquez, Y. Xia, J.E. Sader, G.V. Hartland, J. Chem. Phys. 126 (2007) 094709.
[8] J. Wang, C. Guo, Phys. Rev. B 75 (2007) 184304.
[9] M. Hu, X. Wang, G.V. Hartland, P. Mulvaney, J.P. Juste, J.E. Sader, J. Am. Chem. Soc. 125 (2003) 4925.
[10] G.V. Hartland, Phys. Chem. Chem. Phys. 6 (2004) 5263.
[11] W. Huang, W. Qian, M.A. El-Sayed, J. Phys. Chem. B 109 (2005) 18881.
[12] A.H. Zewail, Annu. Rev. Phys. Chem. 57 (2006) 65.
[13] J. Tang, D.S. Yang, A.H. Zewail, J. Phys. Chem. C 111 (2007) 8957.
[14] J. Tang, J. Chem. Phys. 128 (2008) 164702.
[15] J. Tang, Appl. Phys. Lett. 92 (2008) 011901.
[16] N. Del Fatti, C. Voisin, F. Chevy, F. Vallee, C. Flytzanis, J. Chem. Phys. 110 (1999) 11484.
[17] C. Voisin, N. Del Fatti, D. Christofilos, F. Vallee, Appl. Surf. Sci. 164 (2000) 131.
[18] T.H.K. Barron, J.G. Collins, G.K. White, Adv. Phys. 29 (1980) 609.
[19] J.H. Hodak, A. Henglein, G.V. Hartland, J. Chem. Phys. 111 (1999) 8613.
[20] J.H. Hodak, I. Martini, G.V. Hartland, Chem. Phys. Lett. 284 (1998) 135.
[21] R.G. Benito, P.S. Isabel, M.L.M. Luis, J. Phys. Chem. B 110 (2006) 11796.
[22] K.J. Bikash, R.C. Retna, J. Phys. Chem. C 111 (2007) 15146.
[23] K.L. Kelly, E. Coronado, L.L. Zhao, G.C. Schatz, J. Phys. Chem. B 107 (2003) 668.
[24] L. Novotny, R.X. Bian, X.S. Xie, Phys. Rev. Lett. 79 (1997) 645.
[25] R. Zadoyan, H. Ye. Seferyan, A.W. Wark, R.M. Corn, V.A. Apkarian, J. Phys. Chem. C 111 (2007) 10836.
[26] P. Yu, J. Tang, S.H. Lin, J. Phys. Chem. C 112 (2008) 17133.